PHYSICAL REVIEW B VOLUME 15, NUMBER 12 15 JUNE 1977

Analysis of electron inelastic-scattering data with application to Cu

L. A. Feldkamp, L. C. Davis, and M. B. Stearns
Research Staff, Ford Motor Company, Dearborn, Michigan 48121
(Received 27 December 1976)

The reduction of electron inelastic-scattering data to a form which can be compared to results of optical experiments and to band calculations is discussed. An improved and efficient method of calculating plural scattering is described and applied to a measured spectrum. Various aspects of surface scattering are discussed, especially as they pertain to the analysis procedure. Results, including dielectric constants, for Cu are shown and are compared to band calculations.

I. INTRODUCTION

Certain features of electron inelastic-scattering (energy-loss) experiments performed in transmission geometry can be interpreted with little, if any, processing of the data. In general, however, it is necessary to process the data considerably before comparing to optical data or band-structure calculations. Among the reasons for this are the following:

(i) Electron scattering experiments essentially measure the quantity $g_2(E) = \mathrm{Im}[-1/\epsilon(E)]$, where $\epsilon = \epsilon_1 + i\epsilon_2$ is the complex dielectric constant. Even when (for small wave vector) ϵ is taken to be the same quantity as determined optically, the relation between structure in $\mathrm{Im}(-1/\epsilon)$ and that in either ϵ_1 or ϵ_2 is not straightforward, except in special cases. One example where it is straightforward is structure due to excitation of core electrons.[1-7] Here $\epsilon_1 \approx 1$ and ϵ_2 is small, so that $\mathrm{Im}(-1/\epsilon) = \epsilon_2/(\epsilon_1^2+\epsilon_2^2) \approx \epsilon_2$ (but see Refs. 3 and 8). Another simple case involves well-defined plasmons.[9,10] Here the energy-loss peak arises from the conditions $\epsilon_1 \approx 0$ and $\epsilon_2 \ll 1$ and often dominates the spectrum.

(ii) The high scattering probability for electrons results in non-negligible plural scattering for moderate electron energies, even for relatively thin films. This necessitates a correction before $\mathrm{Im}(-1/\epsilon)$ can be determined.

(iii) Scattering from the film surfaces can be surprisingly large, even for relatively thick films. In materials which have free-electron-like bands (e.g., Al), such scattering is well defined (as excitation of surface plasmons) and fairly localized in energy. In other cases, perhaps most, structure from surface scattering is closely mixed with that from the bulk, necessitating a correction.

In this paper we describe a method, based on Kramers-Kronig (KK) analysis (Sec. II) for the reduction of energy-loss data to a form which can be compared easily to calculations and other experiments. The principal difference between our method and those which have been presented before[9-12] lies in a more precise and efficient treatment of plural scattering (Sec. III). As an example, we apply this treatment to a measured Cu spectrum in Sec. IV. In Sec. V we consider various effects not included in the simplest formulation of surface scattering. Finally, in Sec. VI, we present results of our KK analysis for Cu.

II. KRAMERS-KRONIG ANALYSIS

The KK analysis which we use is similar to that discussed in detail in Ref. 10; hence we will confine ourselves largely to listing the relevant expressions.

We deal with the complex quantity $g(E)$ defined by

$$g(E) = g_1(E) + ig_2(E) = 1 - 1/\epsilon(E) , \tag{2.1}$$

where $E = \hbar\omega$. The real part of $g(E)$ is related to the imaginary part through

$$g_1(E) = 1 - \mathrm{Re}[1/\epsilon(E)] = (2/\pi)\mathcal{P}\int_0^\infty \frac{g_2(E')E'\,dE'}{(E'^2 - E^2)} . \tag{2.2}$$

Letting $E = 0$, we obtain a sum rule on $g_2(E)$:

$$1 - \mathrm{Re}[1/\epsilon(0)] = (2/\pi)\mathcal{P}\int_0^\infty \frac{g_2(E')\,dE'}{E'} . \tag{2.3}$$

For metals $\mathrm{Re}[1/\epsilon(0)] = 0$. Once (2.2) has been used to infer $g_1(E)$ from $g_2(E)$, we may obtain $\epsilon(E)$ from (2.1). We also compute the quantities

$$n_g(E) = (m/2\pi^2e^2N\hbar^2)\int_0^E E'g_2(E')\,dE' \tag{2.4}$$

and

$$n_\epsilon(E) = (m/2\pi^2e^2N\hbar^2)\int_0^E E'\epsilon_2(E')\,dE' , \tag{2.5}$$

where N is the atom density. These may nonrigorously[13] be regarded as the effective number of electrons contributing to the excitation spectrum up to energy E. The integrand of (2.5), viz.,

$$f(E) = (m/2\pi^2 e^2 N\hbar^2) E\epsilon_2(E) , \tag{2.6}$$

is proportional to the real part of the optical conductivity and may be identified as the density of oscillator strength per unit energy interval. In the limit $E \to \infty$, both quantities n approach the atomic number, and (2.5) is seen to be a restatement of the f-sum rule.[13] It may be shown that any smooth function $g_2(E)$ which tends to 0 as E goes to both 0 and ∞ and which is normalized according to (2.3) {with $\mathrm{Re}[1/\epsilon(0)] = 0$} will produce quantities n defined by (2.4) and (2.5) which tend toward each other as $E \to \infty$. Hence we may check the numerical accuracy of the computation by insuring that n_g and n_ϵ tend to the same value at high energy.

For comparison with optical data, one may compute such quantities as the refractive index

$$\tilde{N} = n + ik = \epsilon^{1/2} , \tag{2.7}$$

the absorption coefficient

$$\mu = (2\omega/c)k = (2E/\hbar c)k , \tag{2.8}$$

and the reflection coefficient (normal incidence)

$$R = [(n-1)^2 + k^2]/[(n+1)^2 + k^2] . \tag{2.9}$$

III. MULTIPLE SCATTERING

The calculation of multiple (single plus plural) scattering of electrons has been the subject of much work.[14-17] Some treatments[10,12] emphasize double scattering, while others, primarily those[15-17] which restrict themselves to elastic scattering, treat all orders of scattering. The present method resembles the latter, but has been extended to apply to inelastic scattering.

We begin by defining $S_1(E, \theta)$ as the probability of single scattering per unit film thickness, energy interval, and solid angle. For the moment we include only volume scattering and assume that S_1 can be represented by the factored form[9]

$$S_1(E,\theta) = (2\pi^2 a_0 E_0)^{-1} g_2(E)/(\theta^2 + \theta_E^2) , \tag{3.1}$$

where E_0 is the incident electron energy, E is the energy lost by the scattered electron, a_0 is the Bohr radius, and $\theta_E = E/2E_0$. Note that we neglect the wave-vector variation of ϵ over the angular region in which S_1 is used in the calculation. We also define a total interaction probability per unit thickness, S_t, such that the probability of not interacting in thickness t is given by $e^{-S_t t}$.

We may then write down an integral equation for the quantity $\bar{S}(x,E,\theta)$, which we define as the probability per unit solid angle and unit energy transfer that an electron will scatter at least once with total deflection θ and energy loss E in traveling a distance x into the film:

$$\bar{S}(x,E,\theta) = xS_1(E,\theta)e^{-S_t x} + \int_0^E \int_{\Omega'} \int_0^x \bar{S}(x',E',\theta') S_1(E-E',\theta'') \times e^{-S_t(x-x')}\, dx'\, d\Omega'\, dE' , \tag{3.2}$$

where θ'' is given by

$$\theta'' = \cos^{-1}(\hat{\Omega}\cdot\hat{\Omega}') \tag{3.3}$$

and we have used the notation $\hat{\Omega} = (\sin\theta\cos\phi, \sin\theta\sin\phi, \cos\theta)$. The first term of (3.2) describes electrons which, in traveling the distance x, scatter exactly once with the specified E and θ and avoid all other processes. The second term sums over all plural scatterings in which an electron scatters at least once with accumulated energy loss E' and deflection θ' in arriving at x', scatters once more with energy loss $E - E'$ and deflection θ'' in dx' about x', and then travels the distance $x - x'$ with no further interactions. We can eliminate the attenuation factors from (3.2) by defining

$$S(x,E,\theta) = e^{S_t x}\bar{S}(x,E,\theta) . \tag{3.4}$$

Thus

$$S(x,E,\theta) = xS_1(E,\theta) + \int_0^E \int_{\Omega'} \int_0^x S(x',E',\theta') S_1(E-E',\theta'') \times dx'\, d\Omega'\, dE' . \tag{3.5}$$

We have regarded the paths of the electrons of interest (those which we ultimately detect), as sufficiently close to the forward direction that the path length is adequately represented by the distance x. We have also used the property that, apart from the very-low-energy region corresponding to annihilation of phonons, $S_1(E,\theta) = 0$ for $E < 0$. Finally, we have assumed, as usual, that the scatterings of a given electron occur independently.

If the left-hand side of (3.5) is repeatedly substituted into the right-hand side, a series expansion results. If this series is truncated at two terms, one recovers essentially the method discussed by Daniels *et al.*[10] Rather than employ such an expansion, we solve (3.5) as an integral equation. The number of integrals involved makes direct integration of (3.5) unwieldy. Consequently we take advantage of the axial symmetry implicit in the scattering described by (3.1) and expand in Legendre polynomials.

We write

$$S(x,E,\theta) = \sum_L s_L(x,E) P_L(\cos\theta) \tag{3.6}$$

and

$$S_1(E,\theta)=\sum_L a_L(E)P_L(\cos\theta)\ . \tag{3.7}$$

Inserting these in (3.5) and applying the addition theorem,[18] we get

$$s_L(x,E)=xa_L(E)+\int_0^x dx'\int_0^E dE'\,a_L(E-E')[4\pi/(2L+1)]\times s_L(x',E')\ . \tag{3.8}$$

It is convenient to define $s_L^P(x,E)$ by

$$s_L(x,E)=xa_L(E)+s_L^P(x,E)\ , \tag{3.9}$$

which, when substituted into (3.8), gives

$$s_L^P(x,E)=[4\pi/(2L+1)]\tfrac{1}{2}x^2\int_0^E dE'\,a_L(E-E')a_L(E')+[4\pi/(2L+1)]\int_0^E dE'\,a_L(E-E')\times\int_0^x s_L^P(x',E')dx'\ . \tag{3.10}$$

In order to determine the coefficients $a_L(E)$, we recognize that $\theta^2+\theta_E^2$ in (3.1) is actually an approximation to $\theta_E^2+2(1-\cos\theta)$ (see Ref. 9). We then utilize the expansion[19]

$$[2(1+\theta_E^2/2-\cos\theta)]^{-1}=\sum_L \tfrac{1}{2}(2L+1)P_L(\cos\theta)Q_L(1+\tfrac{1}{2}\theta_E^2)\ , \tag{3.11}$$

where the Q_L are Legendre functions of the second kind.[18,19] In this way we obtain

$$a_L(E)=(2\pi^2a_0E_0)^{-1}g_2(E)\tfrac{1}{2}(2L+1)Q_L(1+\tfrac{1}{2}\theta_E^2)\ . \tag{3.12}$$

The integral equation (3.10) may be solved numerically by dividing the range of energy, $E_{\max}$, into I intervals and the thickness t into J intervals. We write (3.10) in discrete form for successive values of j, using the trapezoidal rule in the x integration. We then subtract the resulting expressions and utilize (3.12), thus obtaining a form convenient for calculation:

$$\begin{aligned}s_L^P(x_j,E_i)=s_L^P(x_{j-1},E_i)&+\pi[(2L+1)/2][(j^2-(j-1)^2)/I^2J^2]\\&\times[E_{\max}/(2\pi^2a_0E_0)^2]\sum_{i_1=1}^{i-1}t^2g_2(E_{i-i_1})g_2(E_i)Q_L(1+\theta_{E_{i-i_1}}^2/2)Q_L(1+\theta_{E_{i_1}}^2/2)\\&+[\pi/IJ][E_{\max}/2\pi^2a_0E_0]\sum_{i_1=1}^{i-1}tg_2(E_{i-i_1})Q_L(1+\theta_{E_{i-i_1}}^2/2)[s_L^P(x_j,E_{i_1})+s_L^P(x_{j-1},E_{i_1})]\ ,\end{aligned} \tag{3.13}$$

where $E_i=iE_{\max}/I$ and $x_j=jt/J$. With the assumption that plural scattering is negligible at the lowest energy, (3.13) may be used recursively to obtain $s_L^P(x_j,E_i)$ for all i, j and L. Note that $s_L^P(x_j,E_i)$ depends on $s_L^P(x_{j'},E_{i'})$ previously computed. The angular distribution of the plural scattering may be expressed as

$$S^P(t,E,\theta)=\sum_L s_L(t,E)P_L(\cos\theta)\ . \tag{3.14}$$

Since, in the present application, we wish to determine detected intensities of single and plural scattering, we define a resolution function. We assume the latter to be factorable in angle and energy, and take the energy part to be narrow in comparison with structure in $s_L(x,E)$. We then expand the angular resolution function, assumed axially symmetric, as follows:

$$R(\theta)=R_0\sum_L r_LP_L(\cos\theta)\ . \tag{3.15}$$

R_0 represents the fraction of the incident beam intensity I_0 which would be collected in the absence of a target if the system were set to detect electrons which had neither changed direction nor transferred energy. The coefficients r_L are simply computed by recursion for Gaussian or Lorentzian shapes (see Appendix A). If the resolution is not axially symmetric, (3.15) can still be used but the r_L themselves depend on the angular setting of the spectrometer and are somewhat tedious to compute. Applying expansions (3.6), (3.7), (3.15), and the addition theorem to integrals of the form

$$I_1(E,\theta)=I_0e^{-s_1t}\,t\int_{\Omega'}S_1(E,\theta')R[\cos^{-1}(\hat\Omega\cdot\hat\Omega')]d\Omega'\ ,$$

we may express the single and plural scattering intensities as

$$I_1(E,\theta)=I_0R_0e^{-s_1t}\,t\sum_L\frac{4\pi}{(2L+1)}a_L(E)r_LP_L(\cos\theta) \tag{3.16a}$$

$$=I_0R_0e^{-s_1t}(2\pi^2a_0E_0)^{-1}tg_2(E)F(\theta,E)\ , \tag{3.16b}$$

and

$$I_P(E,\theta) = I_0 R_0 e^{-S t^t} \sum_L \frac{4\pi}{(2L+1)} s_L^P(t,E) r_L P_L(\cos\theta) . \tag{3.17}$$

The quantity $F(E,\theta) = 2\pi \sum_L r_L P_L(\cos\theta) Q_L(1+\frac{1}{2}\theta_E^2)$ expresses the combined effect of the angular distribution of the scattering function [cf. (3.1)] and the angular resolution function. To the extent that $g_2(E)$ varies slowly with angle, $F(E,\theta)$ predicts the measured angular distribution of single scattering. At fixed angle of measurement, it largely controls the shape of the observed spectrum relative to $g_2(E)$; this aspect has been discussed in Ref. 10.

Some remarks of a practical nature are in order here. The number J of intervals used in the x integration is analogous (though not equivalent) to the number of terms kept in a series expansion of (3.5). The required J depends on the target thickness, the spectrometer angle, and the nature of $g_2(E)$. For the data processed here, $J = 10$ was more than adequate. Because of the generally smooth nature of plural scattering, it is often acceptable to use a fairly coarse energy mesh and to interpolate the plural scattering in between.

The expansion (3.6) implies that we must evaluate the left-hand side of (3.13) for all values of L. Inspection of (3.11) and the fact that θ_E for typical E_0 and E may be in the range 0.000 01–0.01 reveals that convergence will occur only at rather large L (perhaps several thousand). This might seem to pose an insurmountable practical problem, but since a_L, s_L, Q_L, and r_L all vary slowly with L, we may simply divide the required L range into a moderate number of intervals (10 to 20) and use a representative L from each. It is expedient to allow the intervals to increase in size with increasing L. The presence of the r_L in (3.17) has a beneficial effect on the convergence of the computation of $I_P(E,\theta)$.

The method just discussed may be compared to those described in detail by Daniels *et al.*[10] and Wehenkel.[12] We account for all orders of scattering, rather than stopping at double or triple scattering. The properties of the Legendre polynomials allow us to avoid much of the labor involved in handling the angular variables correctly, rather than, for example, approximating the double scattering as a simple convolution in energy of the single scattering intensities [cf. Eq. (11) of Ref. 12]. Since we in effect calculate the angular distribution of the plural scattering and then apply the resolution function to determine what part is collected, our method lends itself to realistic treatment of spectrometer resolution; the work of dealing with possibly complicated angular resolution is concentrated in a single calculation of the r_L, which can then be stored.

We may generalize the foregoing method to include surface scattering if we use the Ritchie[20] form

$$S_1^s(E,\theta) = (2\pi^2 a_0 k_0 E_0)^{-1} \frac{\theta}{(\theta^2+\theta_E^2)^2} \operatorname{Im} \frac{(1-\epsilon)^2}{\epsilon(\epsilon+1)} \tag{3.18}$$

as the probability of scattering from one surface per unit energy interval and solid angle. Equation (3.18) assumes normal beam incidence on the target and neglects retardation as well as interaction of the film surfaces; we discuss these effects in Sec. V.

Considering surface scattering to take place precisely at the surface, we may generalize (3.5). For $0 < x \leq t$

$$S(x,E,\theta) = xS_1(E,\theta) + S_1^s(E,\theta) + \int_0^E \int_{\Omega'} \int_0^x S(x',E',\theta') S_1(E-E',\theta'') \times dx'\, d\Omega'\, dE' . \tag{3.19}$$

At t^+, beyond the film, we have

$$S(t^+,E,\theta) = S(t,E,\theta) + S_1^s(E,\theta) + \int_0^E \int_{\Omega'} S(t,E',\theta') S_1^s(E-E',\theta'') d\Omega'\, dE' . \tag{3.20}$$

If we expand $S_1^s(E,\theta)$ as in (3.7) with coefficients given by

$$b_L(E) = \tfrac{1}{2}(2L+1) \int_{-1}^{1} S_1^s(E,\theta) P_L(\cos\theta) d\cos\theta \tag{3.21}$$

and redefine $s_L^P(x,E)$ by

$$s_L(x,E) = xa_L(E) + b_L(E) + s_L^P(x,E), \quad 0 < x \leq t \tag{3.22}$$

we may generalize (3.10) to

$$s_L^P(x,E) = \frac{4\pi}{(2L+1)} \tfrac{1}{2} x^2 \int_0^E dE'\, a_L(E-E') a_L(E') + x \int_0^E dE'\, b_L(E') a_L(E-E') + \frac{4\pi}{(2L+1)} \int_0^E dE'\, a_L(E-E') \int_0^x s_L^P(x',E') dx' . \tag{3.23}$$

Using the orthogonality of the Legendre polynomials to perform the angular integration implied in (3.20), we get

$$s_L^P(t^+,E)=s_L^P(t,E)+\int_0^E dE'\, s_L^P(t,E')b_L(E-E') \tag{3.24}$$

and

$$s_L(t^+,E)=ta_L(E)+2b_L(E)+s_L^P(t^+,E)\,. \tag{3.25}$$

IV. EXTRACTION OF SINGLE SCATTERING

In Sec. III we described how to calculate plural scattering, given knowledge of $g_2(E)$ [and $\epsilon(E)$ if surface scattering is to be included]. In practice we have, instead, an observed spectrum from which we desire the extract the bulk single scattering, in order to *determine* $g_2(E)$. If we ignore surface scattering, we may take advantage of the fact that solving (3.13) at energy E_i involves g_2 only at lower energy, so that knowledge of $g_2(E_i)$ for $i=1$ is sufficient to start a recursive process. At each higher energy, (3.17) is used to determine $I_P(E,\theta)$ which is subtracted from the observed intensity to yield $I_1(E,\theta)$. Equation (3.16b) is then applied to extract $g_2(E)$. The difficulty is that both the thickness t and the quantity $\bar{I}=I_0R_0e^{-S}t^t$ must be known. Lacking accurate knowledge of $\bar{I}$, we may proceed by noting that $tg_2(E)$ occurs in (3.13) and (3.16b) always as a product. We estimate a value of $\bar{I}$ and carry out the recursive process, extracting $tg_2(E)$ at each value of energy. When finished, we apply sum rule (2.3) in the form

$$(2/\pi)\int_0^\infty \frac{tg_2(E')dE'}{E'}=t \tag{4.1}$$

to determine t. If t thus inferred is not the known thickness, a new value of $\bar{I}$ must be chosen and the process repeated. A check is provided by extrapolating $g_2(E)$ to $E\to\infty$ and calculating n_g according to (2.4). In Cu, for example, we presume that the data and its smooth tail ($1/E^3$ used here) encompass excitation of all electrons from $3s$ through $4s$, so that $n_g(E\to\infty)$ should be 19. In the present case, n_g is ~10 at $E=150$ eV, the extrapolation accounting for the remaining nine electrons.

Inclusion of surface scattering complicates the procedure, since it depends on $\epsilon(E)$ which in turn depends (see Sec. II) on $g_2(E)$ at all E, and necessitates an iterative procedure, similar to that described by Wehenkel.[12] We first regard all scattering as due to the bulk and carry out a removal of plural scattering as described above. Together with a KK analysis, this produces a first estimate of $\epsilon(E)$, from which, with the Ritchie formula, we calculate an estimate of the surface single scattering. The sum of calculated bulk single scattering, surface single scattering, and plural scattering is then compared with the observed spectrum and new estimates of $g_2(E)$ and $\epsilon(E)$ are obtained. From these the plural and surface scattering components are recalculated and the procedure is repeated until the observed spectrum is closely enough reproduced by the sum of its components.

In Fig. 1 we show such a decomposition for data from a relatively thick, nearly-single-crystal Cu film. The primary energy E_0 was 20 keV and the scattering angle θ was 0. We extrapolated the data to $E=0$ using optically measured[21,22] dielectric constants to estimate $g_2(E)$ in the low-E region. Plural-scattering processes which involve a surface scattering were ignored. Observe that in this spectrum plural scattering accounts for most of the scattering at the higher energies; hence derived quantities in this region will be subject to systematic error, though peaks and shapes should be fairly reliable since the plural-scattering correction is smooth. We used the requirement that n_g be near 19 to determine the effective thickness for the film, 980 Å. We found it necessary to use a different effective thickness to characterize surface scattering. This is not unreasonable if the film is not uniform in thickness, since differently weighted averages are operative in the two cases (see Sec. V). Here surface scattering is included as if the film were 500-Å thick, an estimate based on keeping $g_2(E)$ at the low-energy threshold (~2.1 eV) comparable to that inferred from other data we have taken in which the surface scattering is not so prominent. We are well aware of the ar-

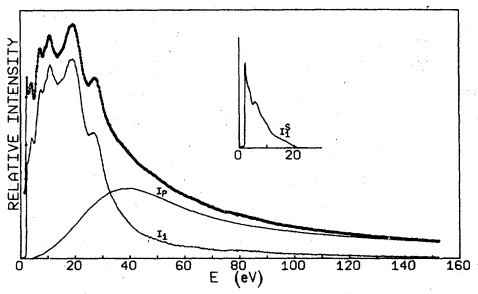

FIG. 1. Decomposition of raw energy-loss data (top curve) for a [100] nearly-single-crystal Cu target into single (I_1), plural (I_P), and surface (I_1^S) scattering components. $E_0=20$ keV, $\theta=0$. The surface scattering component is on the same scale, but has been plotted separately for clarity. The spectrometer energy resolution full width at half maximum (FWHM) is ~0.1 eV; the angular resolution is approximately Gaussian with FWHM $=2\theta_0=0.15°$. The data were taken at 0.16 eV intervals. The peak at 19.2 eV corresponds to 2.19×10^5 counts; the total counting time (sum of 2048 scans) per data point was 20.5 sec. The very-low-energy region, including the elastic peak, is not shown.

bitrariness involved; use of a thinner but more continuous film would improve the situation. Cu is a particularly difficult material for analysis, since its flat d bands ~2 eV below the Fermi level cause the surface scattering to be strongly peaked in the same region where the bulk scattering is increasing rapidly. Our experience with several spectra from both single crystal and polycrystalline films has been that it is difficult to reconcile the apparent levels of surface and plural scattering. In particular, our spectra from polycrystalline specimens generally exhibit much less apparent surface scattering than we would expect, even from continuous films.

V. FURTHER CONSIDERATIONS ON SURFACE SCATTERING

The simple Ritchie form (3.18) contains the essence of the surface contribution and is quite convenient for calculation, since the surface contribution is given as a separate entity from the volume contribution and the dependences on angle and dielectric constant are expressed in factored form. The practical importance of the latter is that (3.18) must be integrated over solid angle, and the factored form allows this integration to be done independently of $\epsilon(E)$. More importantly, the factored form is required for the plural scattering formulation of Sec. III to apply.

Under certain conditions, more elaborate formulations of the surface scattering are necessary. In each case, the desirable properties mentioned above are eliminated. For nonnormal incidence, one must modify (3.18) by a factor[23] which involves the angle of incidence and depends explicitly on the azimuthal angle as well as the polar angle θ. Since this factor diverges in the limit of grazing incidence, the surface contribution may be enhanced greatly if the beam passes at a glancing angle through any region of the specimen. Figure 2 shows the spectrum of a specimen which contained a large number of holes. The details of such spectra depend crucially on the exact position of the beam relative to the target. Note the similarity of this spectrum to the calculated surface spectrum in Fig. 1. It is clear that the surface scattering shown in Fig. 2 overwhelms that due to the bulk. The importance of using continuous films is obvious.

The effects of retardation may be understood qualitatively with reference to a dispersion relation for surface plasmons in a simple metal, such a Fig. 1 of Ref. 24. Inclusion of retardation in the dispersion relation has the effect of forcing the small-wave-vector portion of the ω vs k curve to be asymptotic to the light line, $\omega = ck$. Only if contributions from this region are a sufficiently great fraction of the total surface scattering will the inclusion of retardation be important in the scattering problem; this tends to be the case for relatively low energies, even when (as in Cu) the dispersion relation is more complicated or ill defined. The effects of the interaction of the film surfaces are important in the same energy region and may be understood in the same way. Kroger[25] has derived a formula which includes both of these effects. In his formula the volume and surface contributions are often heavily intertwined, e.g., the individual contributions may have large negative excursions. As we see from Fig. 3, the difference between the spectra calculated for Cu from the Kroger and Ritchie formulas is appreciable only at low energy. We feel that, in this case, the difference is smaller than other uncertainties associated with calculation of surface scattering.

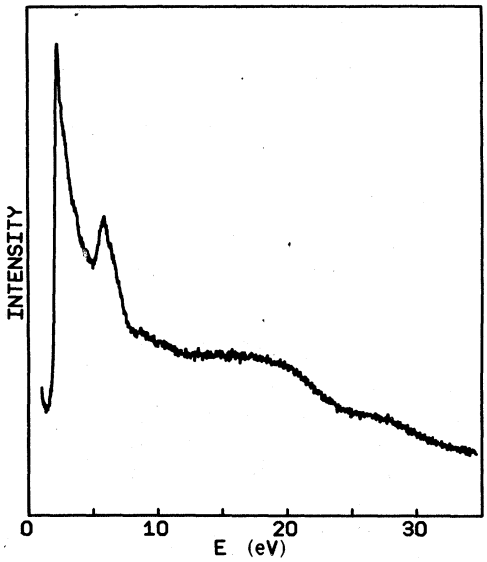

FIG. 2. Example of raw data from a [100] Cu target observed to contain numerous pinholes.

Because of their exposure to air, our Cu films are expected to be covered by thin oxide layers, probably $CuO_{0.67}$.[26] A reasonable estimate for the thickness is 25 Å.[27] In order to assess the possible effect of such a layer on each side of the film, we have performed the straightforward but tedious extension of the Ritchie procedure (neglecting retardation) to derive the scattering probability for a composite three-region specimen. The results are given in Appendix B. As a test of this formulation, we applied it to aluminum. It is well known that the presence of an oxide layer shifts the surface plasmon in a free-electron metal to a lower frequency; in Al the shift is from $\hbar\omega/\sqrt{2} \approx 10$ eV to ~7 eV. In Fig. 4 we compare a portion of an

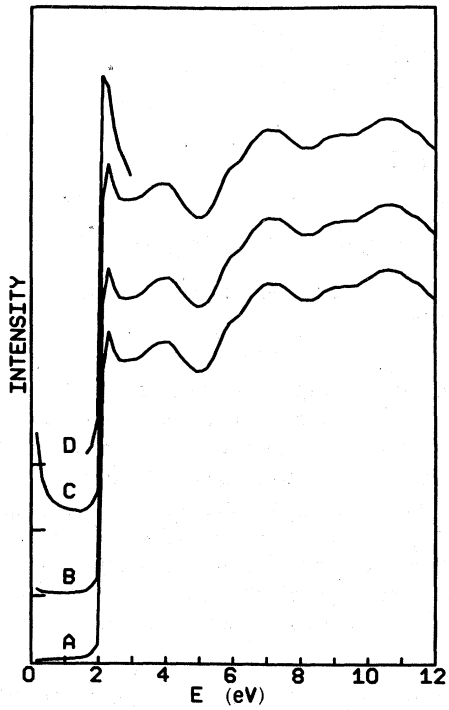

FIG. 3. Single (bulk plus surface) scattering profiles for 500-Å Cu based on the dielectric constants of Fig. 6: (a) Ritchie formula for surface scattering; (b) effect of interaction of surfaces included, retardation neglected; (c) Kroger formula; (d) effect of 25-Å $CuO_{0.67}$ layers using ϵ_0 derived from Ref. 26; no retardation. Successive curves have been displaced for clarity.

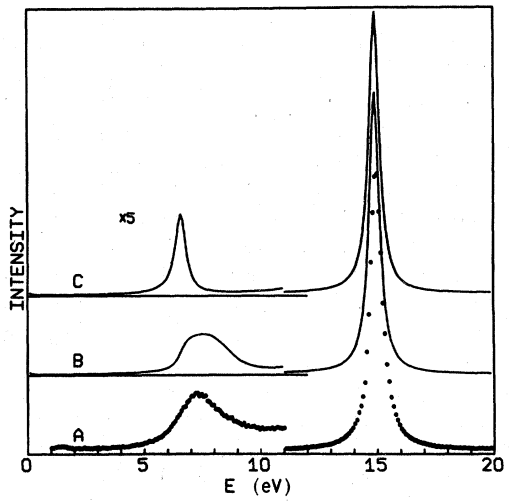

FIG. 4. Comparison of observed and calculated surface and volume plasmons in Al: (a) Experimental data, $E_0 = 18$ keV; (b) calculated with Drude form (values from Ref. 28: $E_p = 14.9$ eV; $E_\gamma = 0.53$ eV) for 500-Å thick Al with 25-Å layers of $\epsilon_0 = 4.1$ oxide on each side; (c) same as (b), but oxide taken as infinitely thick.

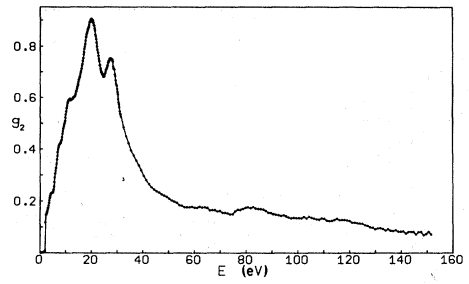

FIG. 5. Function $g_2(E) = \mathrm{Im}[-1/\epsilon(E)]$ for Cu determined from the data of Fig. 1. Beyond ~ 30 eV the points have been grouped to reduce scatter.

experimental Al spectrum (a) with results of calculations based on a simple Drude model.[13] The dielectric constant of the oxide was taken as 4.1.[28] Note that the broadened nature of the experimental surface plasmon is reproduced by the calculation which treats the oxide as finite (b), while taking the oxide to be thick (c), as usually is implicitly assumed, results in too sharp a peak.

In Fig. 3 we show a calculation of the total single scattering for oxide-coated Cu over the energy range for which Wieder and Czanderna[26] have given optical constants for $CuO_{0.67}$. We see that the oxide has caused the edge to be enhanced, though the fractional increase in overall intensity is less than 20%.

VI. RESULTS AND DISCUSSION

In Fig. 5 we show $g_2(E)$ for Cu as inferred from the single scattering spectrum shown in Fig. 1. The structure in g_2 is generally similar to that determined by other workers,[10,12,29] though the detailed shape is sensitive to the method of corrections for surface and plural scattering. Plots of $\epsilon_1(E)$ and $\epsilon_2(E)$ as determined by KK analysis are shown in Fig. 6; these are the values we used to compute the surface scattering. The density of oscillator strength $f(E)$, expressed in units of electrons/atom/eV, is shown in Fig. 7.

Before discussing these results, we wish to point out the features we feel are most vulnerable to inaccuracies in the data processing. The height of the low-E threshold in $g_2(E)$ depends on how much surface scattering is subtracted, although normalization through (2.3) reduces the sensitivity. Our value (~0.145) is only slightly larger than that of Daniels *et al.*,[10] but considerably less than that of Wehenkel,[12] whose data seem to contain more surface scattering than he has subtracted. The value of ϵ_2 at its minimum just below 2 eV depends on the low-E extrapolation (see Sec. IV) and consequently is somewhat arbitrary. The value here is slightly lower than that determined

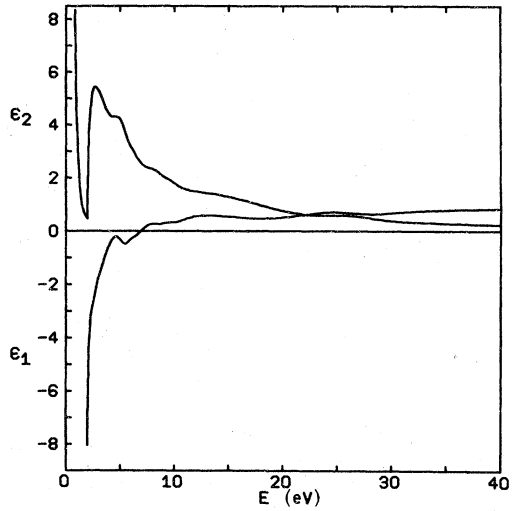

FIG. 6. $\epsilon_1(E)$ and $\epsilon_2(E)$ for Cu derived from $g_2(E)$ of Fig. 5.

optically. As mentioned above, the value at high energy of $g_2(E)$ and, to a greater degree, those of $f(E)$ and the absorption coefficient μ, depend sensitively on the amount of plural scattering which is subtracted. The absorption coefficient for Cu has been measured by Haensel, Kunz, and Sonntag[30] (HKS) and by Hagemann, Gudat, and Kunz (HGK).[31] At the representative energies 80 and 150 eV, HKS measure $\mu = 6.0$ and 4.5×10^5 cm^{-1}, respectively, while HGK obtained 7.7 and 4.5×10^5 cm^{-1}. Our corresponding values are 6.9 and 5.6×10^5 cm^{-1}, almost within the stated error limits (15%) of the HKS experiment.

From Figs. 5–7 we see that there is no well-defined plasmon (ϵ_2 is large where $\epsilon_1 = 0$). The nature of the peaks in $g_2(E)$ between about 10 and 50 eV is complicated, arising from relatively small changes in ϵ_1 and ϵ_2. As noted by Wehenkel,[12] peaks in $f(E)$ in this range occur near minima of $g_2(E)$, though the correspondence is by no means exact. Beyond ~50 eV, $\epsilon_1 \approx 1$ and structure in $g_2(E)$ is also visible in $f(E)$.

The inferred $\epsilon_1(E)$ and $\epsilon_2(E)$ are reasonably close to optical measurements of these quantities.[21,22,32] Our good energy resolution allows the low-energy region of $g_2(E)$ to be determined with greater certainty than in previous energy-loss experiments; indeed, because of the nature of the KK analysis, this region has considerable effect on the values of ϵ_1 and ϵ_2 at higher energies.

In Table I we list the principal features in the curve of oscillator strength density. The general shape of $f(E)$ and the positions of the various peaks are not very sensitive to errors in the data processing. Within the stated uncertainties, the energies quoted in Table I apply whether the surface scattering has been subtracted or not and are the same for a similar analysis of data from a polycrystalline film. Lacking a calculation of $f(E)$ or $\epsilon_2(E)$ over a large energy range, based upon the band structure, we here simply attempt to relate observed features to transitions expected on the basis of band structures calculated by Chen and Segall[33] (parametrized using results of various

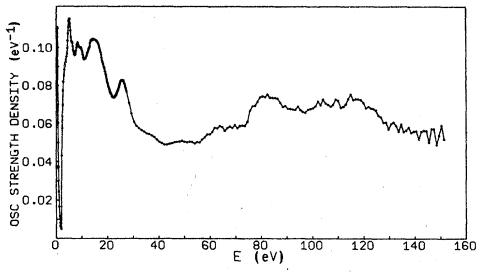

FIG. 7. Plot of the density of oscillator strength $f(E)$ for Cu.

TABLE I. List of features in the oscillator strength density. Unless otherwise specified, positions are believed correct to 0.1 eV, based on consistency with other sets of data.

Feature	Meas. E (eV)	Calc. E (eV) a	b	Assignment
Threshold	2.1	2.1	2.1	$\Delta_5 \rightarrow \Delta_1(E_F)$
		2.1	2.1	$Q_+ \rightarrow Q_-(E_F)$
Peak	5.2	5.0	4.6	$L_{2'} \rightarrow L_1$
		5.3	5.3	$Q_+(L_1^l) \rightarrow Q_-^u(E_F)$
		5.4	5.3	$\Delta_1^l \rightarrow \Delta_1(E_F)$
Minimum	7.1			
Peak	8.4	8.4	8.4	$\Sigma_4 \rightarrow \Sigma_1^u$ (near K)
		8.9	8.6	$W_{1'} \rightarrow W_3$
Peak	9.6	9.7	9.4	$W_1 \rightarrow W_3$
		9.5–9.8		$\Sigma_1^l \rightarrow \Sigma_3$ (near K)
Minimum	11.0			
Maximum	15.0	14.0	13.5	$W_{2'} \rightarrow W_1$
			15.5	$X_2 \rightarrow X_{5'}$
			15.4	$X_5 \rightarrow X_{5'}$
Minimum	22.6 ± 0.5			
Peak	25.9 ± 0.2		27.2	$\Gamma_{12} \rightarrow \Gamma_{15}$
			26.8	$\Gamma_{25'} \rightarrow \Gamma_{2'}$
			26.8	$L_1 \rightarrow L_{2'}$
			27.7	$L_1 \rightarrow L_{3'}$
			24.9	$L_3 \rightarrow L_{2'}$
			25.9	$L_3 \rightarrow L_{3'}$
			23.5	$L_3 \rightarrow L_{2'}$
			24.5	$L_3 \rightarrow L_{2'}$
			26.3	$L_{2'} \rightarrow L_3$
Weak bump 35			33.5	$\Gamma_1 \rightarrow \Gamma_{15}$
Broad edge 74 ± 1				$M_{II,III}(3p \rightarrow 4s)$

[a] From Ref 33.
[b] From Ref 34.

experiments) and Burdick.[34] The low-energy edge in $f(E)$ (a peak in ϵ_2) may be identified with the energy from the d bands to the Fermi level in the [100] direction. Most of the observed peaks result from transitions from the $3d$ levels to p-like states above the Fermi level. Energies and proposed assignments, consistent with dipole selection rules, for the various transitions are listed in Table I. Though the observed structure agrees fairly well with transition energies based on band calculations, a calculation of $\epsilon_2(E)$ [or $f(E)$] would be of great interest, as would a calculation of $g_2(E)$.

The $M_{\mathrm{II,III}}$ edge at ~74 eV is prominent in Fig. 7, even though it hardly shows up on the scale in which the raw data is plotted in Fig. 1. As has been noted previously,[30] the edge is not well defined. The finite lifetime of the core hole, which decays by super-Coster-Kronig (Auger) processes,[35] can account for 2 eV of the width of the edge. The remainder is probably due to the nature[34] of the wave functions above the Fermi level. The Q_-, Z_3, and Δ_1 bands are strongly p-like just above E_F, implying small matrix elements for dipole transitions from $3p$ states. Transitions to the s-like states in bands such as Σ_1, Q_+, and Λ_1 should be larger. Hence the shape of the edge will be influenced by the relative densities of p-like and s-like states.

ACKNOWLEDGMENTS

We wish to thank Dr. S. Shinozaki for preparing the Cu and Al films upon which data were taken and Professor B. Segall for a useful discussion.

APPENDIX A

We wish to compute the coefficients r_L, where

$$r_L = (1/R_0)\tfrac{1}{2}(2L+1)\int_{-1}^{1} R(\theta)P_L(\cos\theta)d\cos\theta. \quad \text{(A1)}$$

For Lorentzian resolution,

$$R(\theta) = R_0\theta_0^2/(\theta^2+\theta_0^2). \quad \text{(A2)}$$

Using

$$\theta^2+\theta_0^2 \approx 2(1+\theta_0^2/2-\cos\theta) \quad \text{(A3)}$$

and[19]

$$\int_{-1}^{1}(z-x)^{-1}P_L(x)dx = 2Q_L(z)\ , \quad \text{(A4)}$$

we get

$$r_L = [(2L+1)/2]\theta_0^2 Q_L(1+\tfrac{1}{2}\theta_0^2)\ . \quad \text{(A5)}$$

The Q_L may be computed using the same recursion relation which applies to the Legendre polynomials P_L.[18]

For Gaussian resolution,

$$R(\theta) = R_0\exp[-(\ln 2/\theta_0^2)\theta^2]$$
$$\approx R_0\exp(-\lambda)\exp(\lambda\cos\theta)\ , \quad \text{(A6)}$$

where $\lambda = 2\ln 2/\theta_0^2$. Then

$$r_L = \tfrac{1}{2}(2L+1)\exp(-\lambda)\int_{-1}^{1}\exp(\lambda\cos\theta)P_L(\cos\theta)d\cos\theta$$
$$\equiv \tfrac{1}{2}(2L+1)M_L\ . \quad \text{(A7)}$$

The coefficients M_L may be determined by recursion.[36] For λ large,

$$M_0 = \lambda^{-1}\ ,$$
$$M_1 = \lambda^{-1}(1-\lambda^{-1})\ , \quad \text{(A8)}$$
$$M_{L+1} = -[(2L+1)/\lambda]M_L + M_{L-1},\quad L>1\ .$$

APPENDIX B

We give here an expression for the scattering probability, neglecting retardation, for a three-region film of thickness $2b$ in vacuum. The center section, of thickness $2a$, has dielectric constant $\epsilon(E)$. The outer regions are each taken to be of thickness $(b-a)$ and to have dielectric constant $\epsilon_0(E)$. The method we used was the same as that employed by Ritchie[20] and Kroger.[25]

We obtain

$$S_1(E,\theta) = (e^2/\pi^2\hbar^2v^2)(k_0^2/\phi^2)$$
$$\times \mathrm{Re}\{-i[2\epsilon_0^{-1}(b-a)+2\epsilon^{-1}a]$$
$$+\lambda s^{-1}\{-b_1\exp(isb)/u_2 - b_5\exp(-isb)/u_1 + b_3(-2i/\phi^2)(\lambda\sin sa - s\tanh\lambda a\cos sa)$$
$$+c_3(2/\phi^2)(\lambda\tanh\lambda a\cos sa + s\sin sa) + (h_1+b_3)(f_{4s}+f_{2s})$$
$$+(h_2+c_3\tanh\lambda a)(f_{4s}-f_{2s}) + (\epsilon/\epsilon_0)[c_3(f_{4c}+f_{2c}) + b_3\tanh\lambda a(f_{4c}-f_{2c})]\}\},$$

where k_0 is the wave vector and v the velocity corresponding to an electron of energy E_0. Other quantities which appear in the above are defined as follows:

$$\lambda = k_0\theta\ ,$$
$$s = \omega/v\ ,$$
$$\phi^2 = s^2+\lambda^2\ ,$$

$$u_1 = is + \lambda ,$$

$$u_2 = is - \lambda ,$$

$$d_1 = \cosh\lambda(b-a) + \epsilon_0 \sinh\lambda(b-a) ,$$

$$d_2 = \sinh\lambda(b-a) + \epsilon_0 \cosh\lambda(b-a) ,$$

$$h_1 = (\epsilon_0^{-1} - \epsilon^{-1}) \cos sa ,$$

$$h_2 = i(\epsilon_0^{-1} - \epsilon^{-1}) \sin sa ,$$

$$b_3 = [(\epsilon_0^{-1} - 1) \cos sb - d_1 h_1]/[d_1 + (\epsilon/\epsilon_0) d_2 \tanh\lambda a] ,$$

$$c_3 = [i(\epsilon_0^{-1} - 1) \sin sb - d_1 h_2]/[d_1 \tanh\lambda a + (\epsilon/\epsilon_0) d_2] ,$$

$$b_2 = h_1 - h_2 + b_3 - c_3 \tanh\lambda a ,$$

$$b_4 = h_1 + h_2 + b_3 + c_3 \tanh\lambda a ,$$

$$c_2 = (\epsilon/\epsilon_0)(c_3 - b_3 \tanh\lambda a) ,$$

$$c_4 = (\epsilon/\epsilon_0)(c_3 + b_3 \tanh\lambda a) ,$$

$$b_1 = \epsilon_0[-b_2 \sinh\lambda(b-a) + c_2 \cosh\lambda(b-a)] ,$$

$$b_5 = \epsilon_0[-b_4 \sinh\lambda(b-a) - c_4 \cosh\lambda(b-a)] ,$$

$$f_{2\frac{c}{s}} = [\exp(\lambda a)/2u_1][\exp(-au_1) - \exp(-bu_1)] \pm [\exp(-\lambda a)/2u_2][\exp(-au_2) - \exp(-bu_2)] ,$$

$$f_{4\frac{c}{s}} = [\exp(-\lambda a)/2u_1][\exp(bu_1) - \exp(au_1)] \pm [\exp(\lambda a)/2u_2][\exp(bu_2) - \exp(au_2)] .$$

[1] J. L. Robins and J. B. Swan, Proc. Phys. Soc. Lond. 76, 857 (1960).
[2] D. L. Misell and A. J. Atkins, Philos. Mag. 27, 95 (1973).
[3] C. Wehenkel and B. Gauthe, Phys. Status Solidi B 64, 515 (1974).
[4] J. J. Ritsko, S. E. Schnatterly, and P. C. Gibbons, Phys. Rev. B 10, 5017 (1974).
[5] R. E. Dietz, E. G. McRae, Y. Yafet, and C. W. Caldwell, Phys. Rev. Lett. 33, 1372 (1974).
[6] M. B. Stearns and L. A. Feldkamp, AIP Conf. Proc. 29, 286 (1976); M. B. Stearns and S. Shinozaki, Physica B (to be published).
[7] L. C. Davis and L. A. Feldkamp, Solid State Commun. 19, 413 (1976).
[8] L. C. Davis and L. A. Feldkamp, Phys. Rev. B 15, 2961 (1977).
[9] H. Raether, *Springer Tracts in Modern Physics* (Springer, Berlin, 1965), Vol. 38, p. 85.
[10] J. Daniels, C. V. Festenberg, H. Raether, and K. Zeppenfield, *Springer Tracts in Modern Physics* (Springer, Berlin, 1970), Vol. 54, p. 77.
[11] D. L. Misell and A. F. Jones, J. Phys. A 2, 540 (1969).
[12] C. Wehenkel, J. Phys. (Paris) 36, 199 (1975).
[13] F. Wooten, *Optical Properties of Solids* (Academic, New York, 1972).
[14] L. Marton, J. A. Simpson, H. A. Fowler, and N. Swanson, Phys. Rev. 126, 182 (1962).
[15] S. Goudsmit and J. L. Sauderson, Phys. Rev. 57, 24 (1940).
[16] G. Moliere, Z. Naturforsch. A 3, 78 (1948).
[17] H. A. Bethe, Phys. Rev. 89, 1256 (1953).
[18] J. D. Jackson, *Mathematics for Quantum Mechanics* (Benjamin, New York, 1962), Appendix B.
[19] I. S. Gradshteyn and I. M. Ryzhik, *Table of Integrals, Series, and Products* (Academic, New York, 1965), p. 821.
[20] R. H. Ritchie, Phys. Rev. 106, 874 (1957).
[21] P. B. Johnson and R. W. Christy, Phys. Rev. B 6, 4370 (1972).
[22] G. P. Pells and M. Shiga, J. Phys. C 2, 1835 (1969); and private communication.
[23] E. A. Stern and R. A. Ferrell, Phys. Rev. 120, 130 (1960).
[24] E. N. Economou, Phys. Rev. 182, 539 (1969).
[25] E. Kroger, Z. Phys. 216, 115 (1968).
[26] H. Wieder and A. W. Czanderna, J. Appl. Phys. 37, 184 (1966).
[27] S. Roberts, Phys. Rev. 118, 1509 (1960); Willes Weber (private communication).
[28] P. Schmuser, Z. Phys. 180, 105 (1964).
[29] M. Creuzburg, Z. Phys. 196, 433 (1966).
[30] R. Haensel, C. Kunz and B. Sonntag, Phys. Lett. 25A, 205 (1967).
[31] H.-J. Hagemann, W. Gudat, and C. Kunz, J. Opt. Soc. Am. 65, 742 (1975).
[32] H. Ehrenreich and H. R. Philipp, Phys. Rev. 128, 1622 (1962).
[33] A.-B. Chen and B. Segall, Phys. Rev. B 12, 600 (1975).
[34] G. A. Burdick, Phys. Rev. 129, 138 (1963).
[35] L. I. Yin, I. Adler, T. Tsang, M. H. Chen, D. A. Ringers, and B. Crasemann, Phys. Rev. A 9, 1070 (1974).
[36] H. A. Antosiewicz, in *Handbook of Mathematical Functions*, edited by M. Abramowitz and I. A. Stegun (U.S. Dept. of Commerce, Natl. Bur. Stand., Washington, D. C., 1964). Relations 10.2.36 and 10.2.18 on pp. 444 and 445 are used.